

---

I. BARIAKHTAR,<sup>1,2</sup> A. NAZARENKO<sup>1,3,4</sup>

<sup>1</sup>Institute of Magnetism, Nat. Acad. of Sci. of Ukraine  
(36-b, Vernadsky Blvd., Kyiv 03142)

<sup>2</sup>Boston College, Department of Physics  
(140, Commonwealth Avenue, Chestnut Hill, MA 02467, USA)

<sup>3</sup>Department of Physics and Mathematics, NTU "KPI"  
(37, Prosp. Peremogy, Kyiv 03056, Ukraine)

<sup>4</sup>Harvard University, IAM-HUIT  
(1033, Massachusetts Avenue, Cambridge, MA 02138, USA)

## PSEUDOGAP ANOMALIES IN THE NORMAL STATE OF THE ATTRACTIVE HUBBARD MODEL

PACS 74.20.Mn, 74.25.Ha

---

*The normal state temperature one- and two-particle Green's functions are calculated within the framework of the conserving self-consistent approximation accounting for the fluctuations in the particle-particle channel for the attractive Hubbard model. The Padé continuation to the complex plane is used to study the pole structure of the retarded one-particle Green's function. The momentum and temperature dependences of the positions of the leading quasiparticle poles are consistent with Bogolyubov's picture, when the second leading pole emerges and rapidly moves toward the real axis. The non-Fermi liquid behavior of the first leading pole is detected at the intermediate coupling. The two-particle Green's function is used to calculate the temperature dependence of the uniform static spin susceptibility, which is shown to exhibit the diamagnetic tendency, as the system approaches the superconducting phase transition.*

*Keywords:* attractive Hubbard model, one- and two-particle Green's functions, quasiparticle pole.

### 1. Introduction

Angle-resolved photoemission experiments on the high-temperature superconductors have provided the evidence of the presence of the pseudogap in the quasiparticle spectrum above the superconducting transition temperature  $T_c$  [1]. The evidence of the anomalous behavior was first observed on  $\text{Bi}_2\text{Sr}_2\text{CaCu}_2\text{O}_{8+\delta}$  compound [2]. Subsequently, the same feature was observed on other families of the cuprates [3]. This issue has been addressed before, and is closely related, in a broad general context, to the phenomenon of the crossover from the regime of the BCS superconductivity to the Bose–Einstein condensation (BEC) of the preformed pairs [4, 5]. In the

latter, it was considered using the attractive Hubbard model in the range of intermediate couplings, where the Gaussian approximation to the functional integral formulation of the continuum model was considered. The general picture that emerges out of the calculations is presented on Fig. 1. The presence of the pseudogap regime between  $T_c$  and  $T^* > T_c$  is related to the strong pairing fluctuations above the superconducting transition temperature  $T_c$ . At  $T > T^*$ , the conventional Fermi liquid picture is recovered. For a comprehensive review and available analytical results, see [6].

### 2. Diagrammatic Approach

The Gaussian approximation is related to the diagrammatic approach, when the irreducible particle-

particle vertex  $V$  is replaced with the bare potential (see Fig. 2). This completes the set of equations and allows one to obtain the full self-consistent solution for the Green's function [7]. The temperature Green's function has to be analytically continued to the real  $\omega$ -axis to obtain the retarded Green's function, which, in turn, allows one to study the spectral functions of a system:  $\pi A(\mathbf{k}, \omega) = -\Im G^R(\mathbf{k}, \omega + i0^+, T)$ . The conventional method is the Padé approximation [8].

The purpose of this paper is to report on the results of the self-consistent approach in the case of the attractive Hubbard model, which has pairing correlations in the  $s$ -wave channel and the superconductivity in the ground state. The calculations were done in the *normal* state on a two-dimensional square lattice with  $64 \times 64$  sites. The maximum number of Matsubara frequencies was 512 for the lowest temperature.

The generalized frequency- and momentum-dependent gap equation is necessary to assure that the calculations are done in the normal state of the system ( $T > T_c$ ). Within the accepted approximation at  $T = T_c$ , it reduces to the condition  $\lambda = 1$ , where  $\lambda = |U| \times \chi_{pp}^0(q = 0)$ , and the renormalized particle-particle bubble is defined as  $\chi_{pp}^0(q) = (T/N) \sum_k G(k)G(q-k)$  in the  $s$ -wave case (a similar quantity can be easily introduced for models with different symmetries of the superconducting order parameter and will be addressed in future publications) [9]. At  $T > T_c$ ,  $\lambda < 1$ , which controls being in the normal state. Note that, within the accepted approximation,  $\lambda$  is directly related to the pair susceptibility  $\chi_{pp}(q)$ , which is proportional to  $\lambda/(1-\lambda)$  and exhibits the 2D-XY critical scaling over a large temperature interval. Such analysis was performed using the numerically calculated  $\lambda(T)$  depicted in Fig. 3 [10]. As is seen,  $\lambda < 1$  over the accessed temperature interval.

The Hamiltonian reads

$$H = -t \sum_{\langle ij \rangle, \sigma} (c_{i, \sigma}^\dagger c_{j, \sigma} + \text{h.c.}) - \mu \sum_{i, \sigma} n_{i\sigma} + \frac{U}{N} \sum_{\mathbf{k}, \mathbf{p}, \mathbf{q}} c_{\mathbf{k}\uparrow}^\dagger c_{\mathbf{p}\uparrow} c_{\mathbf{q}-\mathbf{k}\downarrow}^\dagger c_{\mathbf{q}-\mathbf{p}\downarrow}, \quad (1)$$

where  $c_{\mathbf{k}, \sigma}^\dagger$  creates an electron in the state  $\mathbf{k}$  with spin projection  $\sigma$ ,  $n_{i\sigma}$  is the number operator, the sum  $\langle ij \rangle$  runs over the pairs of nearest-neighbor lattice sites,  $U$  is the strength of the potential,  $t$  is the nearest-neighbor hopping amplitude, and  $\mu$  is the chemical potential.

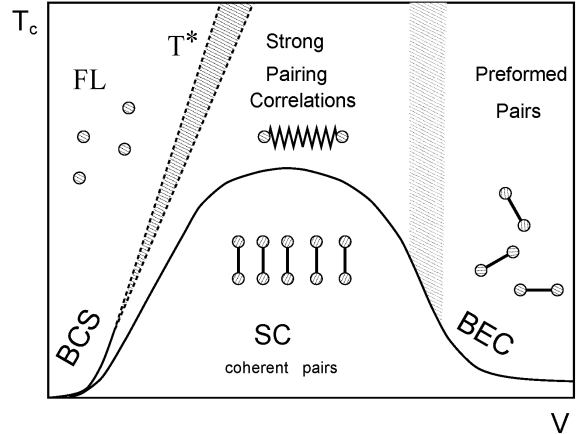


**Fig. 1.** Qualitative temperature-coupling phase diagram of the attractive Hubbard model. The curve with a hump represents the approximate (model-specific) dependence of the critical temperature  $T_c$  on the potential strength  $V$ . The pseudogap regime corresponds to the region between  $T_c$  and  $T^*$ . The acronyms used in the figure are: SC – superconductivity, BEC – Bose–Einstein condensation, BCS – Bardeen–Cooper–Schrieffer (original theory of superconductivity), FL – Fermi liquid

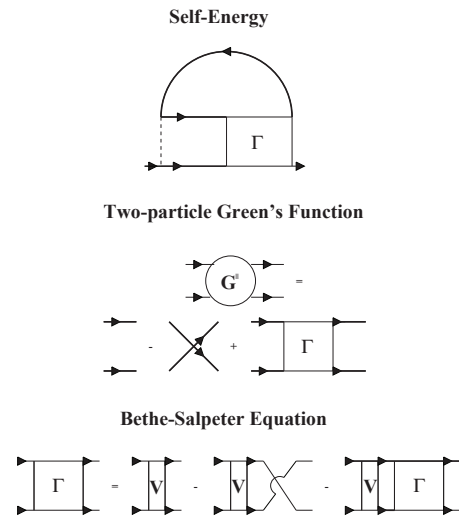


**Fig. 2.** Set of equations for one- and two-particle Green's functions. Note that both Green's functions depend on the same full vertex in the exact treatment, but the set is incomplete [7]

The results discussed in this study were mostly obtained at the intermediate coupling  $U = -4t$  (some results were obtained at  $U = -2t$ ,  $U = -6t$ , and  $U = -8t$  for comparison or contrasting the difference; see the text and figures for details) and the moderate density  $\langle n \rangle = 0.5$  corresponding to the

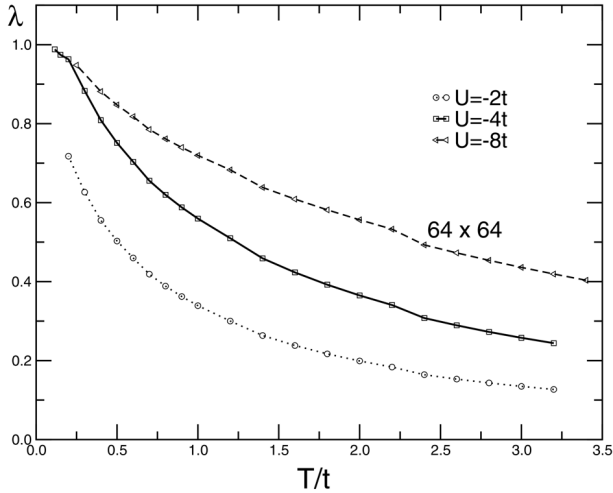


**Fig. 3.** Dependence of the parameter  $\lambda$  (which is directly related to the pair susceptibility  $\chi_{pp}(q)$ , see the text) on the coupling strength for various coupling strengths at the density  $n = 0.5$

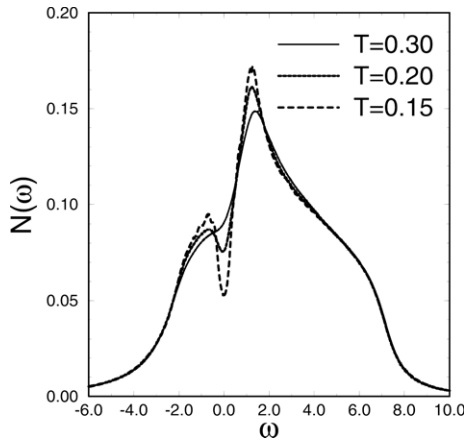


**Fig. 4.** Density of states vs temperature. The pseudogap develops near the chemical potential ( $\omega = 0$ ) as the temperature decreases. Energy unit is  $t$  in this figure

quarter-filled system. The final temperature Green's function was analytically continued to the complex plane, which allowed us to extract the position of leading poles and to study their temperature and momentum behaviors.

The density of states  $N(\omega) = \frac{1}{N} \sum_{\mathbf{k}} A(\mathbf{k}, \omega)$  is plotted in Fig. 4 at various temperatures. This picture agrees with the Monte-Carlo calculations [11] and shows a nontrivial feature of the normal state of the Fermi-system with on-site two-particle attraction:

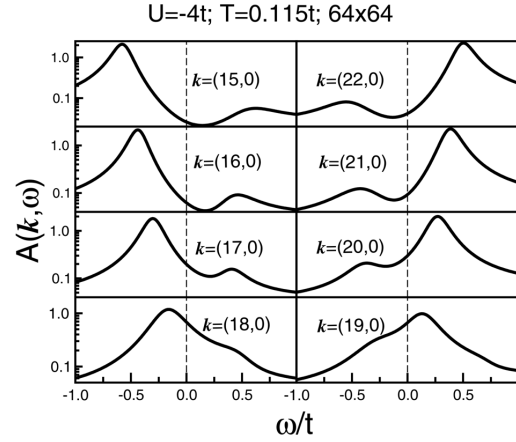


**Fig. 5.** Spectral functions  $A(\mathbf{k}, \omega)$  for various momenta in a vicinity of the non-interacting Fermi surface at  $T = 0.115t$

the depletion of the spectral weight at the chemical potential (in Fig. 4 at  $\omega = 0$ ).

The spectral functions in a vicinity of the non-interacting Fermi surface are shown in Fig. 5 on the log-scale. The momenta are given in terms of  $\pi/32$ . The Fermi momentum corresponds to  $\mathbf{k}_F = (18\pi/32, 0)$ . One can easily notice that the curves have a pronounced two-peak structure: one peak is below, and one is above the Fermi level. Both peaks are evidently overdamped as compared with the conventional Fermi liquid picture.

### 3. Analytic Continuation

To address such puzzling features, the pole structure of the Green's function is studied. Namely, the Padé continuation is performed to the lower complex plane to locate the positions of the leading poles. The Padé approximant can be represented as a series:

$$G(z) \approx \sum_i \frac{R_i}{z - P_i}, \quad (2)$$

and the position  $P_i$  of a pole defines the energy and the lifetime of the one-particle excitation. The analysis of the pole positions shows that, at a low enough temperature, there are only two isolated poles close to the real axis. They define the two-peak structure of the spectral function, while others mostly contribute to the background and are far below in the lower half-plane. The dynamics of the leading poles' motion with temperature is depicted in Fig. 6. The strongest

pole is located at negative frequencies and corresponds to a Landau quasiparticle, which is stable below  $T^*$ . Within the considered temperature interval  $0.1t < T < 0.2t$ , its displacement is negligible. The second leading pole located above the chemical potential is much weaker than the first one and rapidly moves toward the real axis to occupy the position that is consistent with Bogolyubov's excitation.

The remarkable fact that it happens above  $T_c$  testifies to the presence of strong pairing correlations in the normal state. Note that this behavior is not present in the weak-coupling BCS limit. The reason is that, at an intermediate coupling strength, the pair size is much smaller, and, thus, the pair correlations can acquire a considerable strength well before establishing the coherent state.

The incipient pairing instability changes the temperature dependence of the lifetime of a Landau quasiparticle defined as the reciprocal imaginary part of the first pole's position. The inverse lifetime behavior becomes marginal (proportional to  $T$ ) over an extended temperature range. In Fig. 7, the marginal temperature dependence of the position of the leading pole is compared with the 2D Fermi liquid dependence, which can be parametrized as [12]

$$\frac{1}{\tau} = -\frac{\pi}{2} w \frac{T^2}{T_F \alpha} \ln \frac{T}{T_F \alpha}, \quad (3)$$

where  $T_F$  is the Fermi temperature, and  $\alpha$  and  $w$  are fitting parameters. Figure 7 compares two distinct cases:  $U = -4t$  (Fig. 7, a), when the pairing instability in the system creates strong fluctuations associated with it, and  $U = -2t$  (Fig. 7, b) when the system is much less affected by the strength of the superconducting fluctuations in its normal state. The latter case is easily fitted by the 2D Fermi liquid dependence, while the strong coupling case allows for no fitting (note: all cases appear to be linear at the first glance).

Up to now, we have discussed the pseudogap behavior in our approximation in the single-particle Green's function, which carries information about the spectral weight. The results of numerical calculations of the uniform spin susceptibility presented in Fig. 8 were obtained, by using the two-particle Green's function within the framework of the same approximation (see Fig. 2). It shows that the temperature dependence of the spin susceptibility also demonstrates a pseudogap

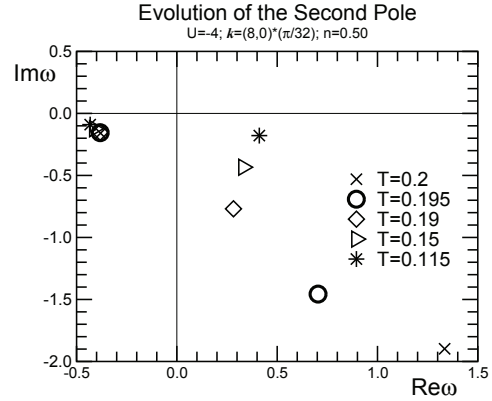
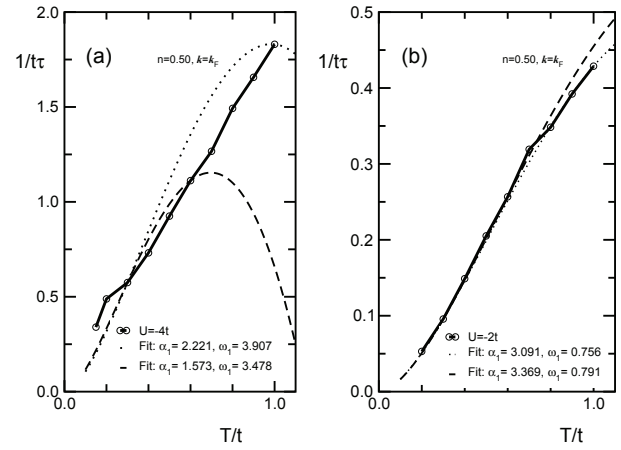


Fig. 6. Motion of two leading poles with decreasing temperature. All energies are given in terms of  $t$



$$1/\tau = -2^* \text{Im} \Sigma(k, \omega) \text{ vs Fermil liquid fit } (\pi/2) \omega (T/T_F \alpha) \ln(T_F \alpha/T)$$

Fig. 7. Marginal temperature dependence of the lifetime of a Landau quasiparticle as compared to the 2D Fermi liquid picture (see the text)

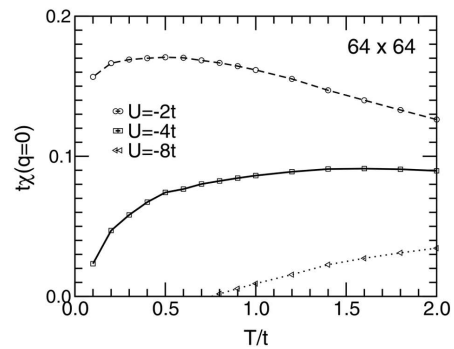


Fig. 8. Temperature dependence of the uniform static spin susceptibility for various coupling strengths at the density  $n = 0.5$

behavior, similar to what is observed in NMR experiments [13]. The pseudogap feature of the spin susceptibility has also been shown to take place in the case of a model, which has the d-wave superconductivity in its ground state. More details of the calculations of the d-wave case will be presented elsewhere [9].

Thus, we have numerically performed the complex plane analysis of the Green's function pole structure of the 2D attractive Hubbard model in the pseudogap regime. The study reveals the marginal (non-Fermi liquid) temperature dependence of the quasiparticle's lifetime and the development of a Bogolyubov-like two-pole structure of the Green's function at low temperatures.

*The authors are sincerely grateful to Prof. Yurii Gorobets for fruitful discussions, comments, and the continuous support of the research.*

*The work was sponsored by the Institute of Magnetism of the National Academy of Sciences of Ukraine and the National Technical University of Ukraine "KPI" of the Ministry of Education and Science of Ukraine.*

1. N.M. Plakida, *High-Temperature Superconductivity: Experiment and Theory*, (Springer, Berlin, 2012).
2. J.-W. Mei *et al.*, Phys. Rev. B **85**, 134519 (2012); N.P. Armitage *et al.*, Phys. Rev. Lett. **87**, 147003 (2001); H. Ding *et al.*, Nature **382**, 51 (1996); Phys. Rev. Lett. **78**, 2628 (1997); A. Loesser *et al.*, Science **273**, 325 (1996).
3. I.M. Vishik *et al.*, New J. of Physics **12**, 105008 (2010).
4. A. Bugrij and V. Loktev, Low Temp. Phys. **35**, 770 (2009).
5. C. Sa de Melo, M. Randeria, and J.R. Engelbrecht, Phys. Rev. Lett. **71**, 3202, (1993).
6. V. Loktev *et al.*, Phys. Rep. **349**, 1 (2001).
7. See, e.g., A.B. Migdal *Theory of Finite Fermi Systems and Applications to Atomic Nuclei* (Wiley, New York, 1967).
8. H.J. Vidberg and J.W. Serene, J. Low Temp. Phys. **29**, 179 (1977).
9. I. Bariakhtar and A. Nazarenko, Research Bulletin of NTUU "KPI", to be published (2014).
10. A. Nazarenko and J.R. Engelbrecht, Europhys. Lett. **51**, 96 (2000).
11. J.M. Singer *et al.*, Phys. Rev. **54**, 1286 (1996).
12. C.M. Varma, in: *Physics of High-Temperature Superconductors* (Springer, Berlin, 1992), p. 137.
13. M. Randeria, N. Trivedi, A. Moreo, and R.T. Scalettar, Phys. Rev. Lett. **69**, 2001 (1992).

Received 18.04.13

*I.В. Бар'яхтар, О.Б. Назаренко*

#### ПСЕВДОЩІЛЬОВІ АНОМАЛІЇ В НОРМАЛЬНОМУ СТАНІ ПРИТЯГАЛЬНОЇ МОДЕЛІ ХАББАРДА

#### Резюме

Одно- і двочасткові температурні функції Гріна нормального стану притягальної моделі Хаббарда розраховуються в рамках самоузгодженого флуктуаційного наближення в каналі частинка-частинка. Аналітичне продовження в комплексну площину було використано для вивчення полюсної структури запізнілої функції Гріна однієї частинки. Імпульсна і температурна залежності позицій провідного полюса квазічастинки узгоджуються з теорією Боголюбова, коли другий ведучий полюс з'являється і швидко рухається в бік реальної осі. Не-Фермі-рідинну поведінку першого ведучого полюса було виявлено в області проміжного зв'язку. Двочасткова функція Гріна була використана для розрахунку температурної залежності рівномірної статичної спінової сприйнятливості, яка проявляє діамагнітні властивості, у міру того, як система наближається до надпровідного фазового переходу.